

Manuscript submitted to Acta Biomaterialia

On May 2016

**3D silicon doped hydroxyapatite scaffolds decorated with elastin-like
recombinamers for bone regenerative medicine.**

Mercedes Vila^{1,2}, Ana García^{1,2}, Alessandra Girotti^{1,3}, Matilde Alonso^{1,3}, Jose Carlos Rodríguez-Cabello^{1,3}, Arlyng González-Vázquez^{1,4}, Josep A. Planell^{1,4}, Elisabeth Engel^{1,4}, Julia Buján^{1,5}, Natalio García-Hondurilla^{1,5}, María Vallet-Regí^{*,1,2}

1. Networking Research Center on Bioengineering, Biomaterials and Nanomedicine (CIBER-BBN), Madrid, Spain.
2. Department of Inorganic and Bioinorganic Chemistry. Faculty of Pharmacy. Universidad Complutense de Madrid. Pza. Ramón y Cajal s/n, E-28040, Madrid, Spain
3. Bioforge Group, University of Valladolid, Edificio LUCIA, Paseo de Belén 19, 47011 Valladolid, Spain.
4. Biomaterials for Regenerative Therapies Group, Institute for Bioengineering of Catalonia (IBEC), and Department of Materials Science and Metallurgical Engineering, Technical University of Catalonia (UPC), Barcelona, 08028, Spain
5. Department of Medicine and Medical Specialities, CIBER-BBN. University of Alcalá. Alcalá De Henares, Spain.

* Corresponding author. Tel: +34 913941843; Fax: +34 913941786.

E-mail address: vallet@ucm.es (María Vallet-Regí)

Abstract.

The current study reports on the manufacturing by rapid prototyping technique of three-dimensional (3D) scaffolds based on silicon substituted hydroxyapatite with Elastin-like Recombinamers (ELRs) functionalized surfaces. Silicon doped hydroxyapatite (Si-HA), with $\text{Ca}_{10}(\text{PO}_4)_{5.7}(\text{SiO}_4)_{0.3}(\text{OH})_{1.7}\text{h}_{0.3}$ nominal formula, was surface functionalized with two different types of polymers designed by genetic engineering: ELR-RGD that contain cell attachment specific sequences and ELR-SNA15/RGD with both hydroxyapatite and cells domains that interact with the inorganic phase and with the cells, respectively. These hybrid materials were subjected to *in vitro* assays in order to clarify if the ELRs coating improved the well-known biocompatible and bone regeneration properties of calcium phosphates materials. The *in vitro* tests shown that there was a total and homogeneous colonization of the 3D scaffolds by Bone marrow Mesenchymal Stromal Cells (BMSCs). In addition, the BMSCs were viable and able to proliferate and differentiate into osteoblasts.

Statement of significance

Bone tissue engineering is an area of increasing interest because its main applications are directly related to the rising life expectancy of the population, which promotes higher rates of several bone pathologies, so innovative strategies are needed for bone tissue regeneration therapies. Here we use the rapid prototyping technology to allow moulding ceramic 3D scaffolds and we use different bio-polymers for the functionalization of their surfaces in order to enhance the biological response. Combining the ceramic material (silicon doped hydroxyapatite, Si-HA) and the Elastin-like Recombinamers (ELRs) polymers with the presence of the integrin-mediate

adhesion domain alone or in combination with SN_A15 peptide that possess high affinity for hydroxyapatite, provided an improved Bone marrow Mesenchymal Stromal Cells (BMSCs) differentiation into osteoblastic linkage.

Keywords.

Bone repair, tissue engineering, Elastin-like Recombinamers (ELRs), silicon doped hydroxyapatite (Si-HA), rapid prototyped 3D scaffolds, Bone marrow Mesenchymal Stromal Cells (BMSCs).

1. Introduction

The 3-D printing technology has given an extra boost to the world of biomaterials in the field of Tissue Engineering, to enable the design and manufacture of prostheses "ad hoc" for each patient. These new manufacturing techniques of biomaterials for clinical use, also give us the ability to toggle various compounds and proteins in the manufacturing process itself and to modify the surfaces of classic biomaterials in a controlled manner. 3D rapid prototyping technique is an emerging method in the scaffold design. It is based on the direct, layer by layer, slow deposition of a ceramic ink to form a three dimensional scaffold. The 3D-plotter used to prepare 3D scaffolds moves along the three directions in space while depositing ink strings over a plate. The plotter movements are controlled by a computer which makes possible to plot very complex 3D structures. This technique has shown that it is possible to prepare 3D scaffolds made of different materials suitable for tissue engineering, for example, chitosan-HA or polylactic acid and polycaprolactone-HA or polyacrylate-HA [1-3].[1,2,3].

A wide application of these materials is based in their ability to induce bone regeneration. The use of grafts is a common technique for filling in bone defects, when it is not possible to use native bone, and they are usually based on hydroxyapatite (HA). Thus, Vallet *et al.* have designed a biomaterial (HA) for use in bone regeneration cavitary defects in tibia of research animals [4][4]. More recently, these materials have evolved thanks to molecular techniques of replacement including silicon (Si) in its structure. These doped with Si (Si-HA), biomaterials are susceptible of being functionalized with different peptides, alone or in combination of two or more of them that would have synergies and may be complementary in function [5][5].

When hydroxyapatite is implanted as bone substitute, the model of wound healing involves the activation of periostium connective tissue which is responsible for the formation of the fibrous capsule surrounding the biomaterial. This capsule does not permit the join between healthy bone ends of the defect. The hydroxyapatite action would cause that surrounding connective tissue became in osteoid tissue, probably due to the action of osteoblasts from healthy areas that colonizing the fibrous capsule and they perform their osteoinductive function onto the fibrous material [6][6]

This means, that the performance of these 3-D biomaterials, when implanted in living tissue, is variable depending on the nature of peptides that are functionalized with. The use of Elastin-like Recombinamers (ELRs) for functionalizing surfaces is a novel advance that has been recently proposed [7][7]. Among the bio-produced polymers, the ELRs, are considered a family with a high potential for biomaterials design.

ELRs are based on repeated sequences, namely “elastomeric domains”, found in an extracellular matrix (ECM) protein, the natural elastin [8,9][8,9]. ELRs retain the elastin mechanical properties, specially its ideal elasticity and outstanding resistance to fatigue [10][10]. Besides, these polymers show unmatched characteristics in terms of biocompatibility [11][11], and combine a strong tendency to self-assemble with an acute smart behaviour, depending on the polymeric architecture and environmental conditions [12,13][12,13]. Additionally, specific functionalities, such as cell-binding sequences that modulate cell adhesion through integrins, and other bioactive functions can be included in their structure by adding several peptide domains derived from different extracellular matrix (ECM) or non-ECM proteins [14,15][14,15].

Several researchers are studying the role of the chemotactic and adhesive RGD peptide, the action appears to induce migration and adhesion of osteoblasts on the surface of the

biomaterial implanted in the defect area, producing a clear improvement of the bone regeneration process [16-18][16,17,18].

In this sense, there is an increasing use of small peptides with antimicrobial properties that enhance the ability of the biomaterials to induce bone regeneration, while preventing the infection caused by their use [19][19]. In this regard, the antimicrobial role of RGD [20][20] and statherin [21][21] are described. Salivary statherin is a small protein of 43 amino acids present in the saliva that exerts its function by regulating tooth mineralization by controlling the deposition of calcium (Ca^{2+}) preventing excessive deposition thereof on tooth enamel [22][22]. The foregoing features having the affinity to bind to the statherin and mineralized HA, through a domain of 15 amino acids located at the N-terminus ($\text{SN}_{\text{A}15}$), this domain exhibits an higher affinity for HAP than the entire statherin molecule due to the negative charge density and helical conformation present in the fragment [23-26][23,24,25,26] and is able to adsorb at hydroxyapatite [22][22]. SN_{15} and its analogous ($\text{SN}_{\text{A}15}$) fragments are ideal candidates for cause and osteoinduction osteogenesis in regenerative processes in bone injuries of varying degrees, as has been well described Tejeda-Montes *et al.* in recent paper on calvarian defect in rat [27][27].

In this paper, we present the possibility of exploiting the ability of certain peptides to enhance bone regeneration process when they are decorated onto 3D scaffolds. For this purpose, the biomaterials are functionalized with chemotactic and adhesive peptides with features such as RGD peptide and the peptide comprising the 15 N-terminal residues of statherin ($\text{SN}_{\text{A}15}$) domain. Therefore, the main objective of our work is the study of bone repair effect of hydroxyapatite doped silicon and functionalized with adhesion peptides (RGD) and/or peptides with high affinity for hydroxyapatite and a marked feature of the process of mineralization ($\text{SN}_{\text{A}15}$).

2. Materials and methods

2.1. Synthesis of Si-HA powder

Nanocrystalline silicon-substituted hydroxyapatite (Si-HA) with the nominal formula $\text{Ca}_{10}(\text{PO}_4)_{5.7}(\text{SiO}_4)_{0.3}(\text{OH})_{1.7}\text{h}_{0.3}$, where h indicates vacancies at the hydroxyl position, was prepared by aqueous precipitation reaction of $\text{Ca}(\text{NO}_3)_2 \cdot 4\text{H}_2\text{O}$, $(\text{NH}_4)_2\text{HPO}_4$ and $\text{Si}(\text{CH}_3\text{CH}_2\text{O})_4$ solutions, as described elsewhere [28][28]. Briefly, a 1 M solution of $\text{Ca}(\text{NO}_3)_2 \cdot 4\text{H}_2\text{O}$ was added to solutions of $(\text{NH}_4)_2\text{HPO}_4$ and $\text{Si}(\text{CH}_3\text{CH}_2\text{O})_4$ of stoichiometric concentration to obtain the composition described above. The mixture was stirred for 12 h at 80 °C. The pH was kept at 9.5 by NH_3 addition. During the reaction the pH was continuously adjusted to 9.5 to ensure constant conditions during synthesis. The precipitated Si-HA powder was treated at 700 °C to remove nitrates without introducing important changes in the structure and microstructure of the materials. Si-HA detailed chemical, structural and microstructural characterization can be found in ref. [28][28].

2.2 Polymer Protein Expression and Purification:

Below are shown the two amino-acid sequences of the ELRs utilized in this work.

ELR-RGD:

{MGSSH~~HHHHHHSSGLVPRGSH~~MESLLP[[(VPGIG)₂(VPGKG)(VPGIG)₂]₂AVTGRGDSPASS[(VPGIG)₂(VPGKG)(VPGIG)₂]₂]₆V} whose molecular weight is 60661 Da.

ELR-SN_A15/RGD:

{MESLLP[[(VPGIG)₂(VPGKG)(VPGIG)₂]₂DDDEEKFLRRIGRFG[(VPGIG)₂(VPGKG)(VPGIG)₂]₂]₄

$[(VPGIG)_2(VPGKG)(VPGIG)_2]_2AVTG\textcolor{red}{RGD}\textcolor{black}{SPASS}[(VPGIG)_2(VPGKG)(VPGIG)_2]_2]_4$

V} whose molecular weight is 80730 Da

ELR genes were constructed by standard genetic engineering techniques. The recombinamer biosynthesis was carried out using *Escherichia coli*-based heterologous expression system and their purification from the bacterial lysate was performed using their temperature responsiveness with cycles of temperature-depending reversible precipitations as described elsewhere [29][29]. Purified ELRs were dialyzed in cold type I water and then freeze-dried.

The purity and molecular weight of ELRs were analysed by FTIR, SDS-PAGE and mass spectroscopy (MALDI-TOF/MS) while, the correctness of sequence was checked by amino-acid analysis and ^1H -NMR. The transition temperature of each recombinamer was measured by Differential Scanning Calorimetry (DSC).

2.3. Scaffolds of Si-HA powder

3-D periodic macroporous scaffolds were prepared via direct write assembly of a Si-HA slurry, using 3-D rapid prototyping printing equipment (envisionTEC 3D BioplotterTM). The slurry was formed by the method described in ref. [30]. Briefly, slow addition under stirring of 29 g of Si-HA powder over a solution formed by 3 g Darvan® 811 (sodium polyacrylate dispersant agent), 2-3 drops of glycerine and 22 mL of aqueous solution formed by methacrylamide (MMA) and N,N'-methylen-bis-(acrylsaeureamid) (MBAA). The slurry obtained was housed in a syringe and deposited through a conical needle (diameter 0.51 mm) at the volumetric flow rate required to maintain a constant x-y table speed ($v = 3 \text{ mm s}^{-1}$). The final dimensions of the scaffolds were a mesh with interconnected cells of 8 mm diameter \times 2 mm height for *in vitro* assays. Once the scaffolds were prepared the organic phase employed during the processing stage was

thermally removed at 600 °C for 6 h. These non-coated scaffolds are denoted Si-HA in the text below.

2.4. Functionalizing the Si-HA scaffolds with elastin-like polymers

Si-HA scaffolds were coated by immersion with two different polymers. An elastin-like polymer contained cell attachment specific sequences (RGD domain), samples named Si-HA-RGD. And an elastin-like polymer designed specifically with both hydroxyapatite binding and cell adhesion domains (HAp adhesion ones; SN_A15 of the Stathenin) and with the cells (RGD domain), samples named Si-HA-SN_A15/RGD.

Solutions of both polymers were prepared in a 1x Phosphate Buffer Solution (PBS). In both cases 10 mg/mL solutions were prepared at 4 °C and were let overnight until complete dissolution of polymers. Afterwards, the scaffolds were immersed on 500 µL each polymer solution for one hour with orbital stirring (100 rpm). Then, the coated scaffolds were rinsed in PBS and dried at 37 °C.

2.5 Scaffolds characterization

The structure and composition of Si-HA scaffolds, undecorated and decorated with elastin-like recombinamers, were determined by X-ray diffraction (XRD) , using a Phillips Pw-1800 diffractometer and Cu K_{α} ($\lambda = 1.5406 \text{ \AA}$) radiation. TG analysis, to evaluate the percentage of ELRs incorporation to Si-HA scaffolds, was carried out in a Perkin-Elmer Pyris Diamond TG/DTA instrument, up to 900°C in air with a heating rate of 5°C/min and a flow rate of 100 mL/min. Surface scanning electron microscopy (SEM) micrographs of Si-HA, Si-HA-RGD and Si-HA-SN_A15/RGD scaffolds were

recorded with a field emission scanning electron microscope (JEOL modelJSM-6335, Tokyo, Ja-pan) at an acceleration voltage of 15 kV.

2.6. *In vitro tests*

2.6.1. *Viability and proliferation test*

Rat Bone marrow Mesenchymal Stromal Cells (rBMSCs) were obtained and processed as described elsewhere [31]. They were cultured on three different biomaterials in order to clarify their effects on viability and proliferation. Particularly, 50000 rBMSCs were seeded on 24 standard well plates TCPS (Tissue Culture Polystyren) or scaffolds containing Si-HA, Si-HA-RGD and Si-HA-SN_A15/RGD placed in non-adherent well plates. It is noteworthy that standard TCPS was used as positive control for viability and proliferation. rBMSCs were cultured during 24 h, 11 and 16 days using osteogenic medium containing Advanced DMEM supplemented with 15 % Fetal Bovine Serum (FBS), 1 % Penicillin/Streptomycin (Pen/Strep), 1% L-Glutamine (L-Glu), 10 mM β -glycerophosphate, 50 μ g/mL ascorbic acid and 10-8 M dexamethasone. Once reached the period of time, cells were lysed using M-PER (Pierce). M-PER was allowed to react during 15 min in a shaker at 4 °C. Afterwards, cellular suspensions were centrifuged at 2500 g during 10 min at 4 °C. The supernatants were stored at -20°C prior to analysis. To estimate the number of cells per sample it was used the cytotoxicity detection kit Lactate dehydrogenase (LDH) manufactured by Roche. This kit is based on the measurement of the LDH activity to quantify the number of cells. Quantification was performed following the instructions of the manufacturer.

2.6.2. *Cell colonization of scaffolds*

50000 rBMSCs transfected with the green fluorescent protein (GFP) were seeded on Si-HA, Si-HA-RGD and Si-HA-SN_A15/RGD and cultured during 3 days using standard

culture medium for BMSCs (Advanced DMEM, 15 % FBS, 1% Pen/Strep and 1% L-Glu). Once reached the culture period images on the top and inside of the scaffolds were acquired using a Leica fluorescent stereomicroscope. To get the inside images scaffolds were transversally split by mean of a scalpel.

2.6.3 Alkaline Phosphatase (ALP) Activity

The alkaline phosphatase (ALP) is a very well-known bone marker involve in the process of bone mineralization. The ALP activity, it was measured by means of the Sensolyte pNPP Alkaline Phosphatase Kit from ANESPEC. Same cellular supernatants obtained in the 2.5.1 section were used as samples in the current assay. Quantification protocol suggested by the manufacturer of the Kit was followed.

2.6.4. Osteocalcin ELISA

As well as ALP, Osteocalcin (OC) plays an important role in bone mineralization, and is a widely known marker for osteoblasts. In order to reveal the differentiation of 50000 rat BMSCs cultured on TCPS, Si-HA, Si-HA-RGD and Si-HA-SNA15/RGD, the Osteocalcin rat ELISA (Demeditec Diagnostic GmbH) was used. OC was measured at 7d, 11d and 16d. To avoid the FBS interference and to synchronize the cells the culture medium was changed 24 h before the measurement. Cells were washed twice with PBS and then osteogenic medium FBS reduced (1% FBS) was added. Once reached the desired period of time, the supernatant was collected and stored at -20°C prior to analysis. The quantification was performed following the protocol provided by the manufacturer.

All *in vitro* assays data are representative of at least three independent experiments, each containing 2-3 replicates, except when otherwise noted. Results are expressed as

the mean \pm SEM. Statistical significance was determined using a two-way analysis of variance followed by a post hoc Bonferroni's correction ($p < 0.05$).

3. Results and Discussion

The efficiency of production and purification were verified through chemical characterizations of the biosynthesized ELRs. FTIR, ¹H-NMR (data not shown) and the SDS-PAGE electrophoresis (Figure 1) of purified ELRs sample confirmed their purity. Figure 2 shows the MALDI-TOF mass spectrum of ELR-SN_A15/RGD, experimental molecular weight found by this technique matches the expected molecular weight of the recombinamer ($M_w = 80730$ Da) within the experimental error, while the peak at 40535 is due to the doubly charged species. The measured amino-acid content of ELR-SN_A15/RGD matched well its theoretical composition (see Table 1). The results of the MALDI-TOF and amino-acid analysis for ELR-RGD can be seen in ref. [32]. Biosynthesis yield of both purified ELRs was about 300 mg/L of bacterial culture.

The utility of Si-doped hydroxyapatite (Si-HA) as an excellent material in the field of bone tissue regeneration has been previously showed due to its biocompatibility, bioactivity and osteoconductivity [33-35]. With the aim to ensure improved biological response in terms of osseointegration and scaffold resorption, ELRs were incorporated to Si-HA scaffolds surface. These bioactive scaffolds based on silicon-substituted hydroxyapatite were prepared via direct write assembly of Si-HA slurry, using 3-D rapid prototyping printing technique. This strategy allows the design of the porous arrangement, thus controlling size, volume and connectivity pattern of the scaffolds, as can appreciate in the Figure S1 (Supporting Information). SEM micrographs of Figure S1 show the morphology and architecture of scaffolds at low and high magnification. The X-ray diffraction pattern obtained on the surface of one rod of Si-HA scaffold (Figure 3) indicates that all the diffraction maxima correspond to the reflections of an apatite phase. As was expected, the incorporation of recombinamers to the scaffold surface does not alter the composition of them because the XRD patterns obtained were

similar. The percentage of ELRs incorporation to Si-HA scaffolds was estimated from thermogravimetric measurements and the values obtained were around 2 per cent. Figure 4 displays the SEM images of the rod surface of Si-HA, Si-HA-RGD and Si-HA-SN_A15/RGD scaffolds, respectively. As can observe, when the scaffold is decorated with ELR-RGD or ELR-SN_A15/RGD, there are a surface morphology changes. The roughness presents in Si-HA scaffold (Fig. 4a) is significantly lower when ELRs are added to surface scaffolds (Fig. 4b and 4c).

The first recombinamer used shows a simpler composition. Its bioactivity and potential for biofunctionalization relies on the presence of the RGD cell adhesion integrin-intermediate domain, derived from human fibronectin. The benefits of such surface treatment on the ceramic compound are evident. The promotion of early osteoblast addition, induced by the presence of RGD domains on the ceramic surface, would speed the 3D colonization and osseointegration of the implant. However, this simple approach is not free of certain risks of lack of efficiency. As the surface functionalization relies on the passive adsorption of the ELR-RGD, two complications might arise. The first one being an insufficient degree of adsorption of the ELR-RGD on the ceramic surface, limiting so its final ability for cell adhesion and rapid and homogeneous osseointegration. Other complication that might take place is due to the highly charged feature of the RGD domain. It could be the case that adsorption on the polar ceramic might preferentially take place by those RGD domains, preventing them to be readily available for cell adhesion and decreasing so their efficiency.

To avoid those two potential complications, a new ELR has been designed and used in this work; namely ELR-SN_A15/RGD. This particular ELR has a diblock architecture in which two different functionalities are associated to both blocks. The first block is quite similar in composition and bioactivity to ELR-RGD. That block contains the RGD

domain and will bear cell-adhesion functionality. The other block contains a different bioactive domain. That is based on the SN_A15 specific sequence found on the human salivary protein statherin.

According to that, the ELR-SN_A15/RGD di-block would make use of the SN_A15 block for active, efficient, strong and massive adsorption of the ELR-SN_A15/RGD on the calcium phosphate surface of the ceramic implant. Being the recombinamer adsorption now driven primarily by the SN_A15 block, the RGD block would be more abundant and free for promoting efficient cell-binding activity on ceramic surface. Therefore, the recombinamer ELR-SN_A15/RGD has been designed as a kind of ideal functional interface between the inorganic phase and the biological (cellular) phase.

In vitro studies will test that working hypothesis by comparing the osseointegration of the bare ceramic scaffold and those scaffolds on which both ELR-RGD and ELR-SN_A15/RGD had been adsorbed. The differential cellular behaviour on the three scaffolds will be used as a test for this working hypothesis.

3.1. Viability and proliferation

Results from the LDH assay demonstrated that the proliferation rates of rBMSCs cultured on Si-HA, Si-HA-RGD or Si-HA-SN_A15/RGD are statistically the same as shown in Figure 5. The most striking result to emerge from the data is that BMSCs were capable of growth on Si-HA, Si-HA-RGD and Si-HA-SN_A15/RGD and the elastomeric components did not affect the proliferation rate.

3.2. BMSCs colonization of scaffolds

The colonization test was performed in order to clarify if rBMSCs are able to colonize the entire scaffold or the cell attachment is limited to the most external layers.

Particularly, in Figure 6 it is shown that rBMSCs were able to colonize homogeneously the entire scaffolds (top and inside views). GFP transfected cells were observed both inside and outside the scaffold with no differences among the Si-HA, Si-HA-RGD or Si-HA-SN_A15/RGD scaffolds. The cells showed spindle like morphology and no differences were observed between the Si-HA scaffolds and the Si-HA with the ELR.

3.3. Differentiation of BMSCs into osteoblasts

In order to evaluate the osteoblast differentiation of rBMSCs it was measured the functional expression of two well-known osteoblast markers (OC and ALP). The Figure 7A are presented the results related with the OC ELISA test, the findings reveal that the peak in the expression of OC was expressed by rBMSCs cultured on Si-HA-SN_A15/RGD (4.01×10^{-8} ng/cell). Particularly, it is remarkably that the maximum expression of OC it was obtained at 7 days of culture, which is an early expression for this protein. These results correlate well with other studies using rat MSC isolated from bone marrow. These cells cultured on TCP with osteogenic media showed peaks of OC, ALP and collagen at 7 days [31]. Similar results have been obtained by others [36][32]. This effect can be correlated to ALP activity Figure 7B shows that the maximum ALP activity (1.92×10^{-5} ng·min/cell) was reached by cells seeded on Si-HA-SN_A15/RGD during 16 days. In contrast with colonization and viability tests, in the ALP activity were observed significant differences between TCPS, Si-HA, Si-HA-RGD and Si-HA-SN_A15/RGD. This finding suggests that even if cells are able to grow in any surface tested, the cell behaviour is different. Current differentiation assays demonstrate a positive effect of Si-HA-SN_A15/RGD guiding the rBMSCs into the osteoblastic lineage [37][33]. This study demonstrated an enhancement on MSC differentiation when cells were cultured on membranes composed by ELR with SN_A15 in absence of osteogenic media. Previous studies with the ELR-RGD correlate well with the results found in this

study and supports that the availability of the RGD motifs to the cells promotes osteoblast differentiation of the rBMSCs [38]. The SN_A15 sequence acts as a mineral nucleator and has affinity for hydroxyapatite. Thus, it is feasible to think that the Si-HA and the 3D structure are a good support for cell proliferation and colonization and that the presence of the ELR with both sequences, SN_A15/RGD, acts as a synergistic effector on MSC differentiation towards osteoblasts. The stiffness of the scaffold would also play a role towards the differentiation of MSC towards mature osteoblasts.

4. Conclusion

In summary, we have developed an innovative scaffold for bone tissue regeneration. Rapid prototyped Si-HA scaffolds have been biofunctionalized by the absorption of the bioactive protein polymers ELRs and the cell-material interaction of mesenchymal stem cells has been studied. The presence of the integrin-mediate adhesion domain alone or in combination with SN_A15 peptide that possess high affinity for hydroxyapatite have not determined an increase of cells proliferation rate and analogous viability was observed. The Si-HA, Si-HA-RGD and Si-HA-SN_A15/RGD scaffolds are able to support the cell culture growth in a similar manner. Instead of that, ability of the three scaffolds of inducing mesenchymal stem cells differentiation into the osteoblastic lineage was statistically different. Differentiation studies reveal a positive effect of Si-HA-SN_A15/RGD guide the mesenchymal stem cells into the osteoblastic lineage which make them excellent candidates for future *in vivo* assays.

Acknowledgements

Authors would like to thank the CIBER-BBN for supporting this work through the SCAFFTIDE Intramural Project. This study was supported by research grants from Ministerio de Ciencia e Innovación (MICINN) through the projects MAT2012-35556, MAT2009-14195-C03-02, European Project HEALTH.2011.1.4-2-278557, CSO2010-11384-E (Aging Network of Excellence), EC (NMP-2014-646075, HEALTH-F4-2011-278557, PITN-GA-2012-317306 and MSCA-ITN-2014-642687), MINECO (MAT2013-42473-R and MAT2013-41723-R) and JCyL (VA244U13 and VA313U14). M. Vila would like to thank the LÓREAL-Unesco Program for Women in Science for funding part of this research and we would like to thank Belén González for her assistance in cell culture.

Figure Captions

Figure 1. SDS-polyacrilamide gel electrophoresis of the purified ELRs. Lane M: Molecular weight standards, numbers on the right indicate the corresponding apparent MW values of the standard proteins (in kDa). Lane 1: purified ELR-RGD. Lane 2: purified ELR-SN_A15/RGD.

Figure 2. Mass spectra (MALDI-TOF/MS) of ELR-SN_A15/RGD.

Figure 3. Digital photograph and XDR pattern of Si-HA scaffold. All the diffraction maxima correspond to the reflections of an apatite phase. The Si-HA-RDG and Si-HA-SN_A15/RGD samples show similar XDR patterns.

Figure 4. SEM micrographs corresponding to surface rods of (a) Si-HA, (b) Si-HA-RDG and (c) Si-HA-SN_A15/RGD scaffolds.

Figure 5. Viability and proliferation assays obtained by LDH activity measurements of BMSCs cultured on TCPS (positive control), Si-HA, Si-HA-RGD and Si-HA-SN_A15/RGD at different times.

Figure 6. rBMSCs transfected with the green fluorescent protein (GFP) were cultured on the scaffolds. Microscopy images were taken at 3 days of culture. Left images correspond to the top side of the scaffold for Si-HA, Si-HA-RGD and Si-HA-SN_A15/RGD. Right images correspond to the inside of the scaffolds. It can be observed that cells colonize equally the outside and the inside of the scaffold. No differences were observed among the different samples.

Figure 7. OC and ALP activity of BMSCs on the TCSP (positive control), Si-HA, Si-HA-RGD and Si-HA-SN_A15/RGD scaffolds after 7, 11 and 16 days of incubation.

Figure S1. SEM micrographs corresponding to Si-HA, Si-HA-RDG and Si-HA-SN_A15/RGD scaffolds: low magnifications of top (a) and lateral (b) views, and high magnifications of surface (c) and inside (d) rods.

Tables

Table 1. Theoretical and measured amino acid compositions of ELR-SN_A15/RGD.

residue	theoretical	measured
Asp	16	16,88
Ser	13	11,27
Glu	9	10,04
Gly	340	334,66
Ala	8	6,77
Val	165	164,41
Met	1	
Ile	132	134,79
Leu	6	8,6
Thr	4	3,23
Phe	8	8,91
Lys	36	37,87
Arg	16	17,19
Pro	165	166,29

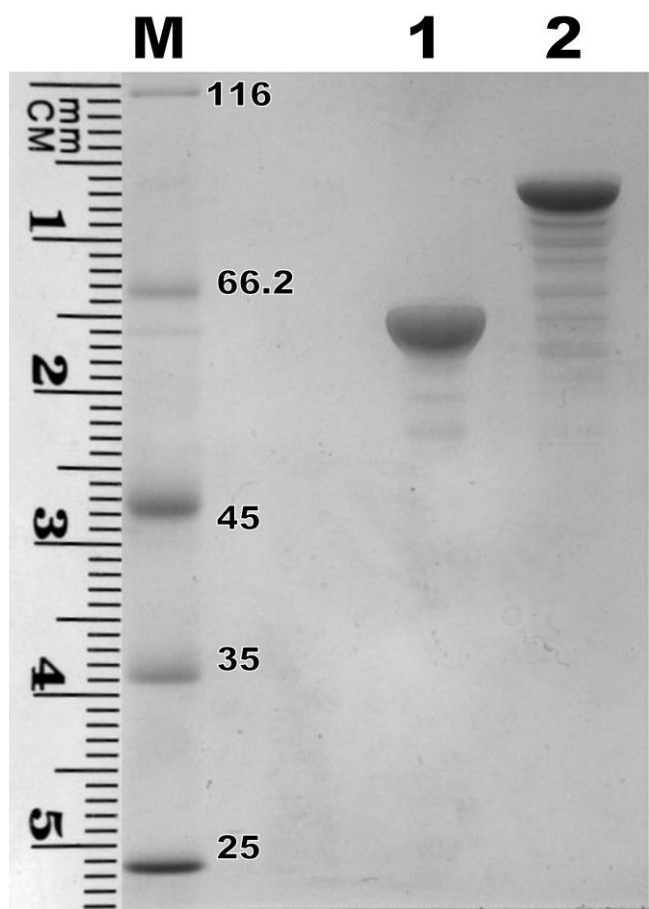


Figure 1

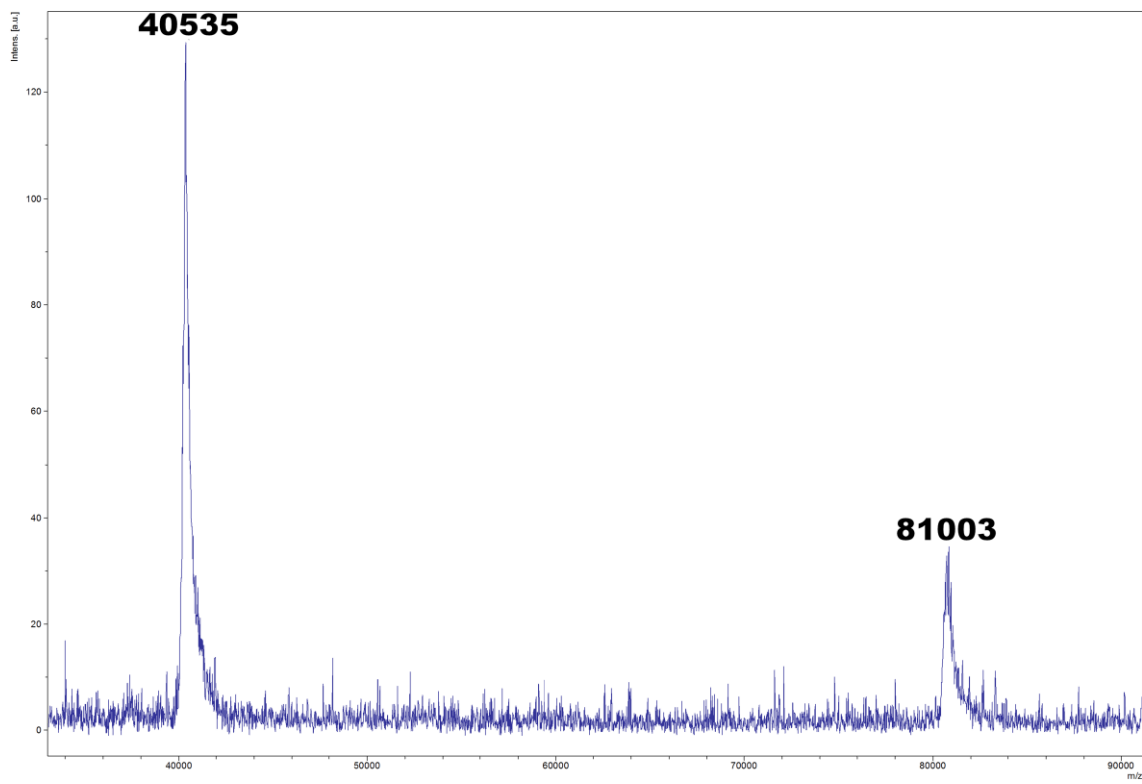


Figure 2

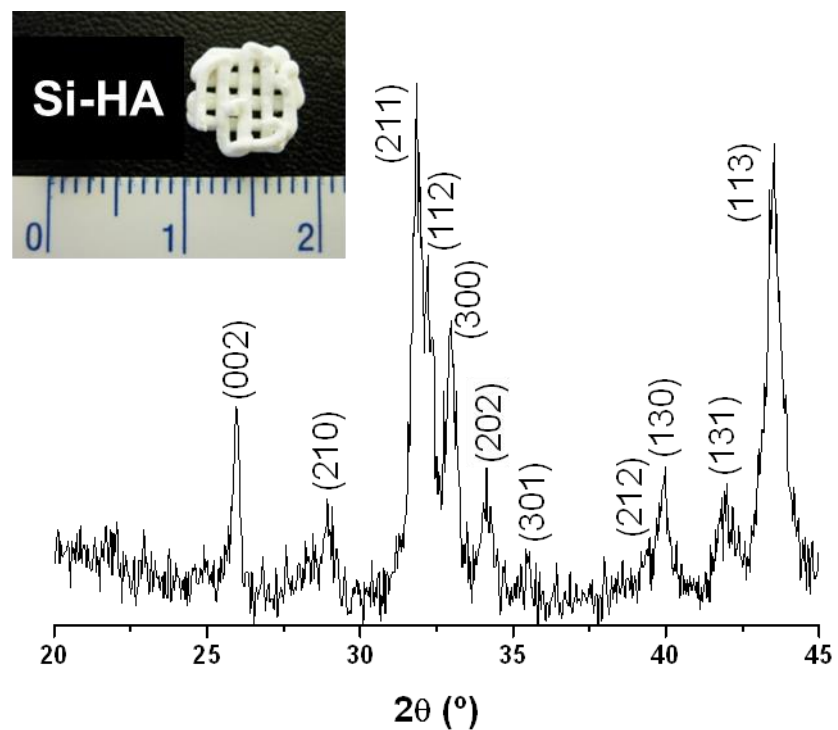


Figure 3

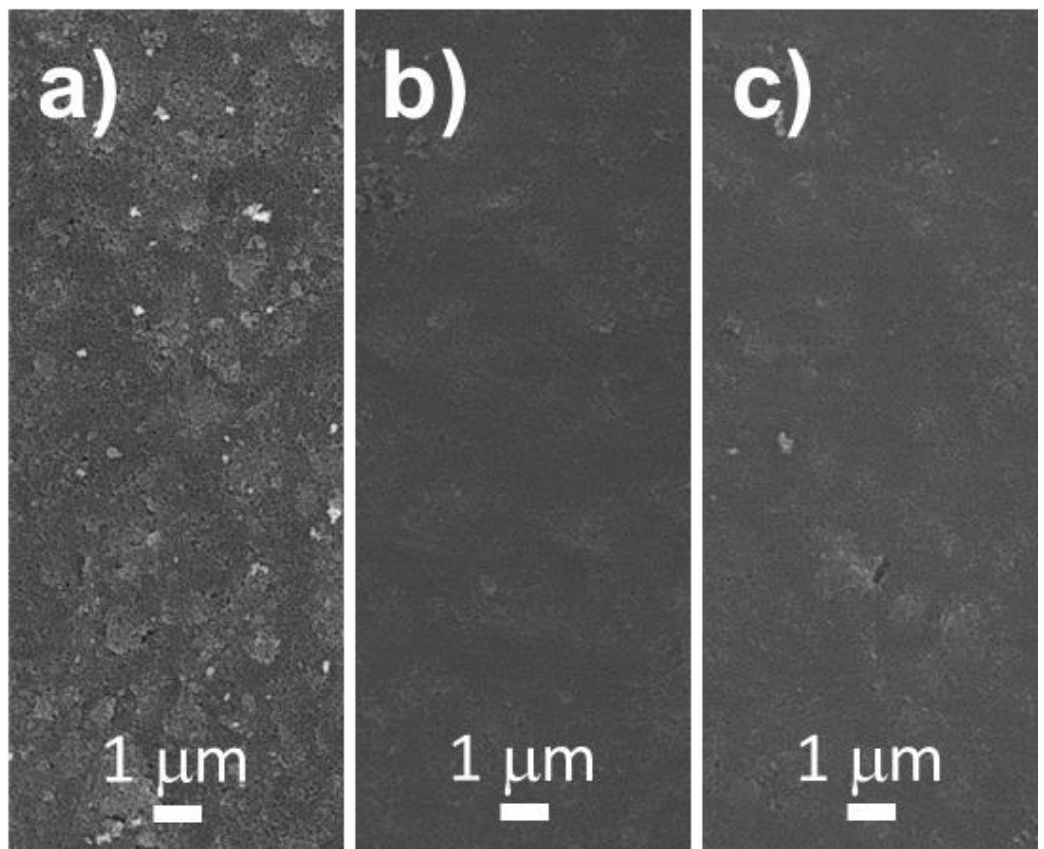


Figure 4

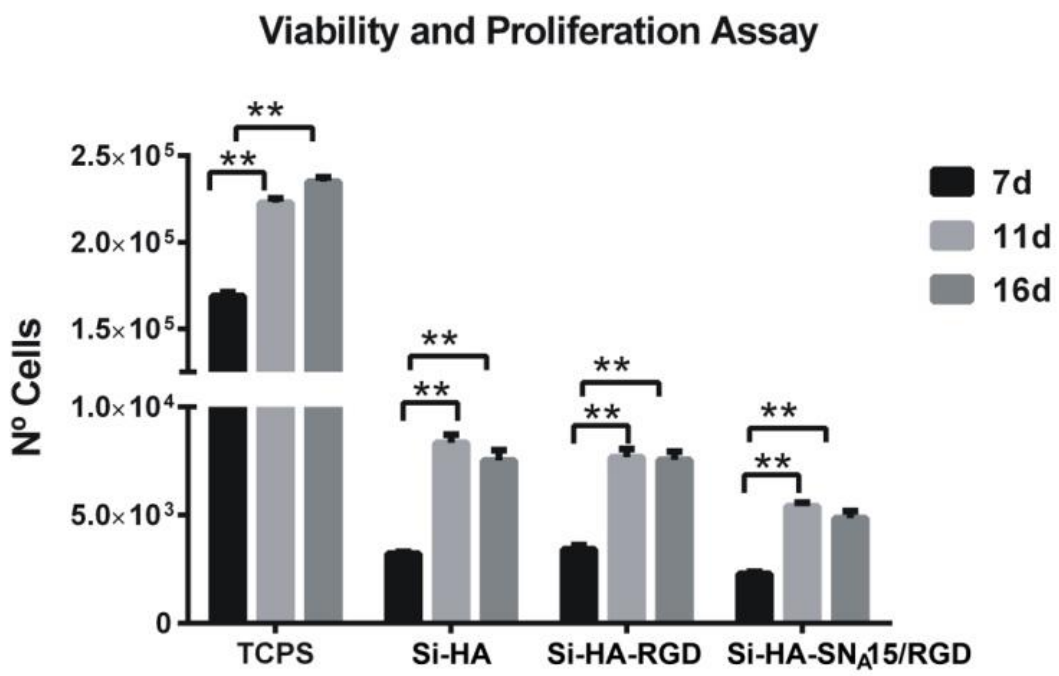


Figure 5

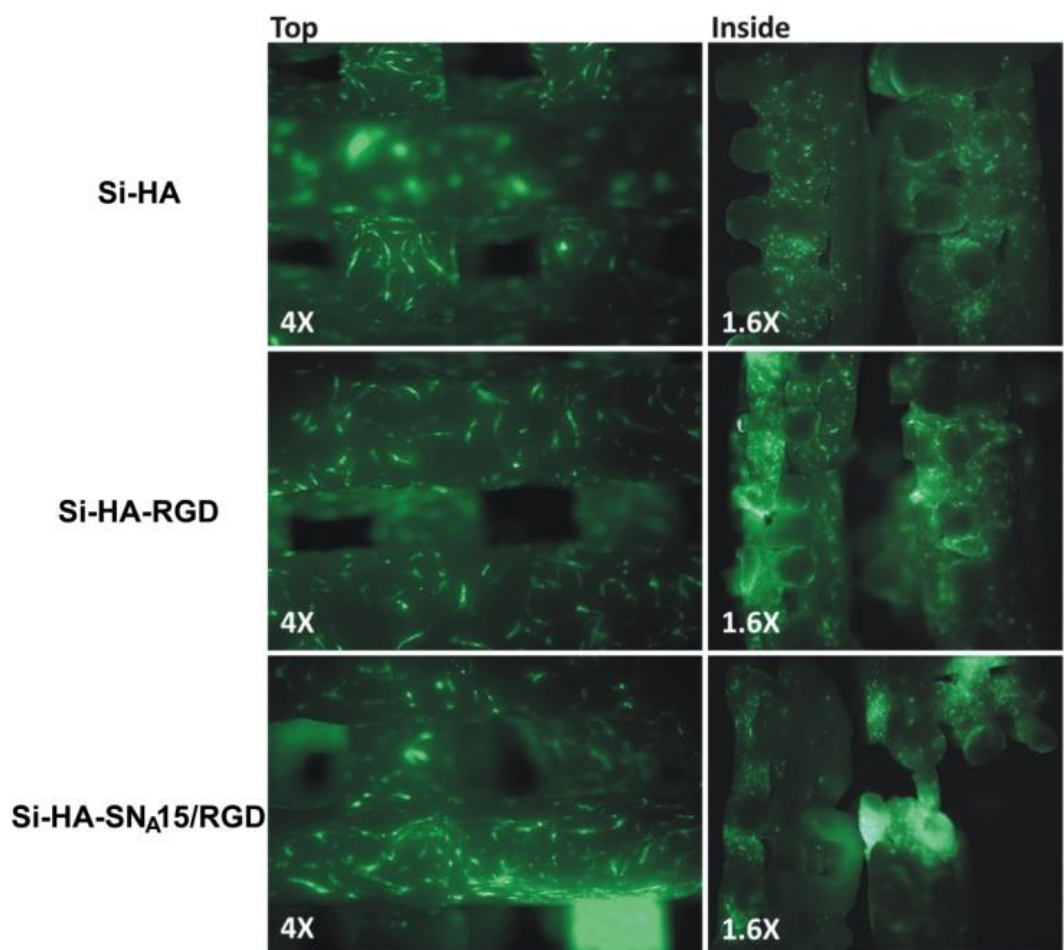


Figure 6

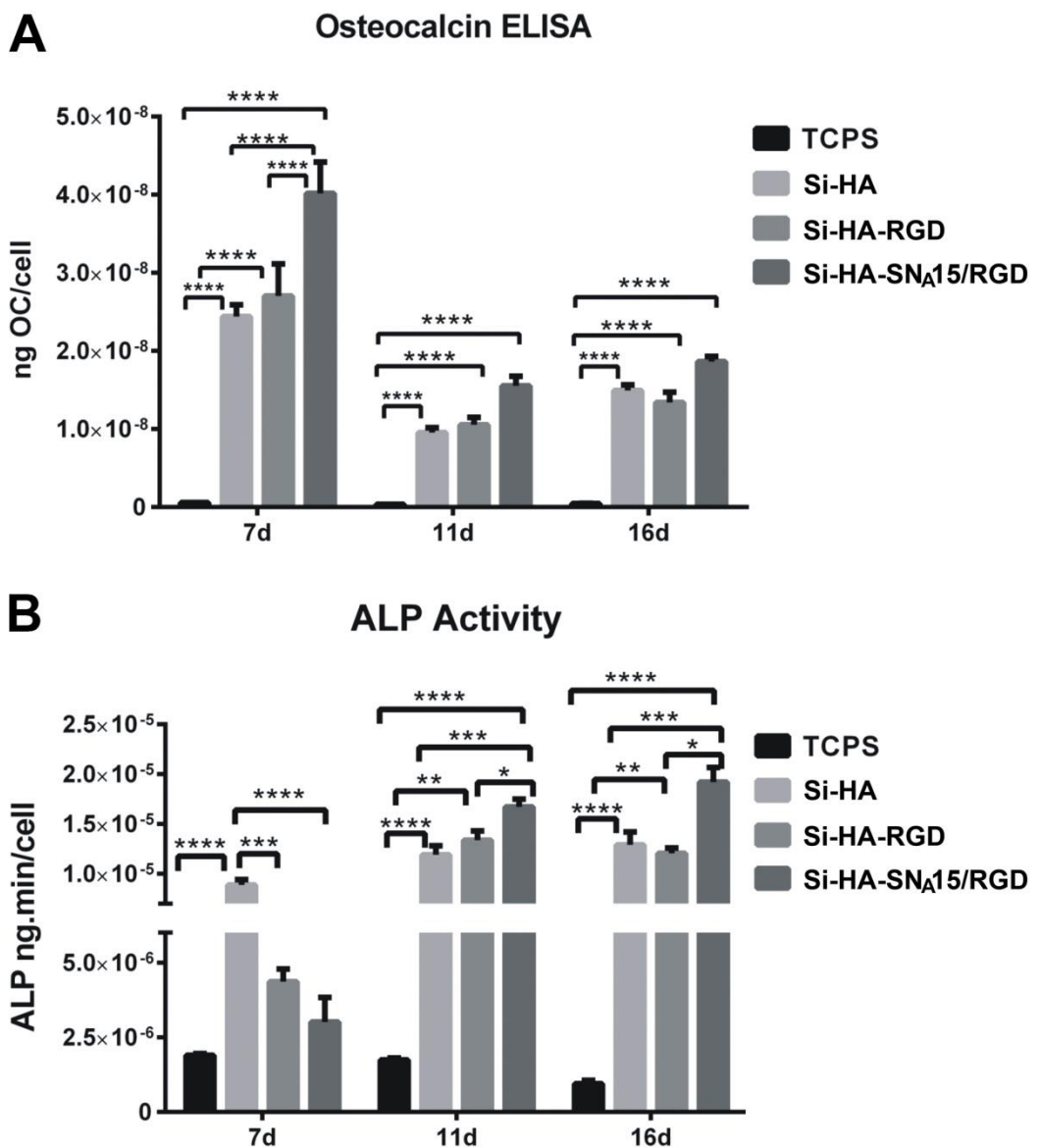
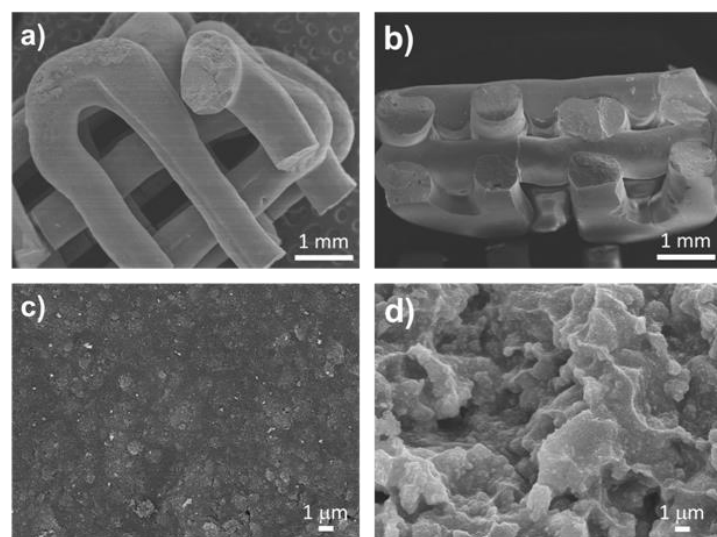
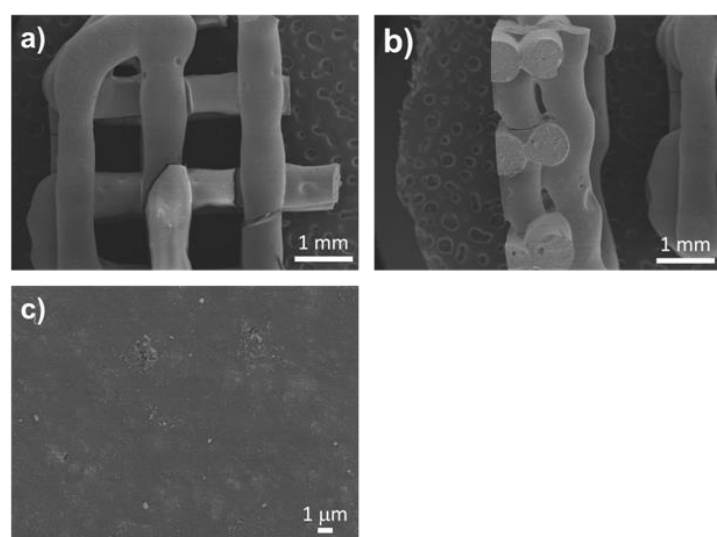


Figure 7

Si-HA



Si-HA-RGD



Si-HA-SN_A15/RGD

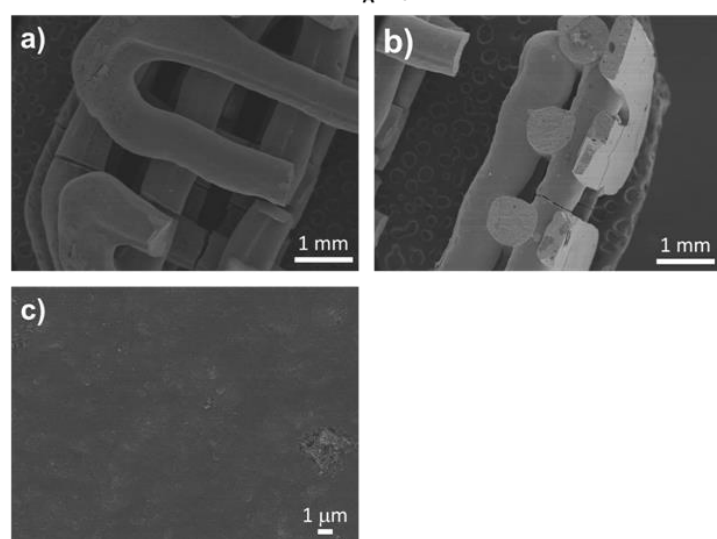
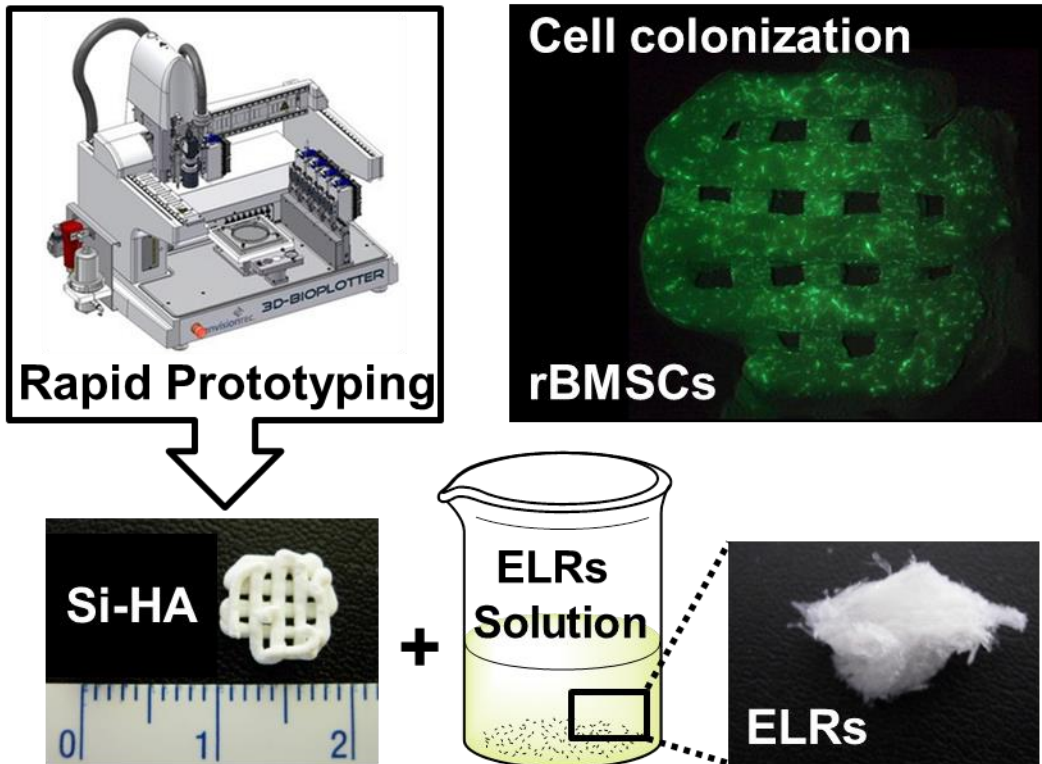


Figure S1.



Graphical Abstract

References

-
- [1] T.H. Ang, F.S.A. Sultana, D.W Hutmacher, Y.S Wong, J.Y.H. Fuh, X.M. Mo, H.T. Loh, E. Burdet, S.H. Teoh. Fabrication of 3D chitosan-hydroxyapatite scaffolds using a robotic dispensing system. Materials Science and Engineering C 20 (2002) 35-42.
- [2] J.G. Dellinger, J. Cesarano, R.D. Jamison. Robotic deposition of model hydroxyapatite scaffolds with multiple architectures and multiscale porosity for bone tissue engineering. J. Biomed. Mater. Res. A. 82 (2007) 383-394.
- [3] J. Russias, E. Saiz, S. Deville, K. Gryn, G. Liu, R.K. Nalla, A.P. Tomsia. Fabrication and *in vitro* characterization of three-dimensional organic/inorganic scaffolds by robocasting. J. Biomed. Mater. Res. A. 83 (2007) 434-445.
- [4] C.G. Trejo, D. Lozano, M. Manzano, J.C. Doadrio, A.J. Salinas, S. Dapía, E. Gómez-Barrena, M. Vallet-Regí, N. García-Hondurilla, J. Buján, P. Esbrit. The osteoinductive properties of mesoporous silicate coated with osteostatin in a rabbit femur cavity defect model. Biomaterials 31 (2010) 8564-8573.
- [5] F.J. Martínez-Vázquez, M.V. Cabañas, J.L. Paris, D. Lozano, M. Vallet-Regí. Fabrication of novel Si-doped hydroxyapatite/gelatine scaffolds by rapid prototyping for drug delivery and bone regeneration. Acta Biomater. 15 (2015) 200-209.
- [6] Y.L. Qu, P. Wang, Y Man., Y.B. Li, Y. Zuo, J.D. Li. Preliminary biocompatible evaluation of nano-hydroxyapatite/polyamide 66 composite porous membrane. Int. J. Nanomedicine 5 (2010) 429-435.
- [7] E. Salvagni, G. Berguig, E. Engel, J.C. Rodríguez-Cabello, G. Coullerez, M. Textor, J.A. Planell, F.J. Gil, C. Aparicio. A bioactive elastin-like recombinamer reduces unspecific protein adsorption and enhances cell response on titanium surfaces. Colloid Surface B 114 (2014) 225-233.

-
- [8] D.W. Urry, T.M. Parker. Mechanics of elastin: Molecular mechanism of biological elasticity and its relationship to contraction. *J. Muscle Res. Cell. Motil.* 23 (2002) 543-559.
- [9] J.C. Rodríguez-Cabello, F.J. Arias, M.A. Rodrigo, A. Girotti. Elastin-like polypeptides in drug delivery. *Advanced drug delivery reviews* 97 (2016) 85-100.
- [10] D.W. Urry, C.H. Luan, C.M. Harris, T. Parker. Protein-based materials with a profound range of properties and applications: The elastin ΔT_t hydrophobic paradigm. *Proteins and modified proteins as polymeric materials* (1997) 133-177.
- [11] R.E. Sallach, W. Cui, F. Balderrama, A.W. Martínez, J. Wen, C.A. Haller, J.V. Taylor, E.R. Wright, R.C. Long Jr., E.L. Chaikof. Long-term biostability of self-assembling protein polymers in the absence of covalent crosslinking. *Biomaterials* 31 (2010) 779-791.
- [12] A. Chilkoti, T. Christensen, J.A. MacKay. Stimulus responsive elastin biopolymers: applications in medicine and biotechnology. *Current Opinion in Chemical Biology.* 10 (2006) 652-657.
- [13] D.W. Urry. Entropic elastic processes in protein mechanisms. II. Simple (passive) and coupled (active) development of elastic forces. *J. Protein Chem.* 7 (1988) 81-114.
- [14] J. Liu, S. Heilshorn, D. Tirrell. Comparative cell response to artificial extracellular matrix proteins containing the RGD and CS5 cell-binding domains. *Biomacromolecules* 5 (2004) 497-504.
- [15] A. Girotti, D. Orbanic, A. Ibáñez-Fonseca, C. González-Obeso, J.C. Rodríguez-Cabello. Recombinant technology in the development of materials and systems for soft-tissue repair. *Advanced healthcare materials* 4 (2015) 2423-2455.

-
- [16] S. Pallu, J.C. Fricain, R. Bareille, C. Bourget, M. Dard, A. Sewing, J. Amédée. Cyclo-DfKRG peptide modulates *in vitro* and *in vivo* behavior of human osteoprogenitor cells on titanium alloys. *Acta Biomater.* 5 (2009) 3581-3592.
- [17] P. Sitasawan, L.A. Lee, K. Li, H.G. Nguyen, Q. Wang. RGD-conjugated rod-like viral nanoparticles on 2D scaffold improve bone differentiation of mesenchymal stem cells. *Front. Chem.* 2 (2014) 1-8.
- [18] X. Zhang, J. Gu, Y. Zhang, Y. Tan, J. Zhou, D. Zhou. Immobilization of RGD peptide onto the surface of apatite-wollastonite ceramic for enhanced osteoblast adhesion and bone regeneration. *Journal of Wuhan University of Technology-Mater. Sci. Ed.* 29 (2014) 626-634.
- [19] M. Kittaka, H. Shiba, M. Kajiya, T. Fujita, T. Iwata, K. Rathvisal, K. Ouhara, K. Takeda, T. Fujita, H. Komatsuzawa, H. Kurihara. The antimicrobial peptide LL37 promotes bone regeneration in a rat calvarial bone defect. *Peptides* 46 (2013) 136-142.
- [20] T. He, Y. Zhang, A.C.K. Lai, V. Chan. Engineering bio-adhesive functions in an antimicrobial polymer multilayer. *Biomed. Mat.* 2015;10(1):015015.
- [21] A.M. Cole, P. Dewan, T. Ganz. Innate antimicrobial activity of nasal secretions. *Infect. Immun.* 67 (1999) 3267-3275.
- [22] P.A. Raj, M. Johnsson, M.J. Levine, G.H. Nancollas. Salivary Statherin: Dependence on sequence charge, hydrogen bonding potency, and helical conformation for adsorption to hydroxyapatite and inhibition of mineralization. *J. Biol. Chem.* 9 (1992) 5968-5976.
- [23] S.S. Schwartz, D.I. Hay, S.K. Schluckebier. Inhibition of calcium-phosphate precipitation by human salivary statherin-structure-activity-relationships. *Calcified Tissue Int.* 50 (1992) 511-517.

-
- [24] A.A. Campbell, A. Ebrahimpour, L. Pérez, S.A. Smesko, G.H. Nancollas. The dual role of poly-electrolytes and proteins as mineralization promoters and inhibitors of calcium-oxalate monohydrate. *Calcified Tissue Int.* 45 (1989) 122-128.
- [25] P.S. Stayton, G.P. Drobny, W.J. Shaw, J.R. Long, M. Gilbert. Molecular recognition at the protein-hydroxyapatite interface. *Crit. Rev. Oral Biol. Med.* 14 (2003) 370-376.
- [26] S. Prieto, A. Shkilnyy, C. Rumplasch, A. Ribeiro, F.J. Arias, J.C. Rodríguez-Cabello, A. Taubert. Biomimetic calcium phosphate mineralization with multifunctional elastin-like recombinamers. *Biomacromolecules* 5 (2011) 1480-1486.
- [27] E. Tejeda-Montes, A. Klymov, M.R. Nejadnik, M. Alonso, J.C. Rodríguez-Cabello, X.F. Walboomers, A. Mata. Mineralization and bone regeneration using a bioactive elastin-like recombinamer membrane. *Biomaterials* 35 (2014) 8339-8347.
- [28] D. Arcos, J. Rodríguez-Carvajal, M. Vallet-Regí. Silicon incorporation in hydroxylapatite obtained by controlled crystallization. *Chem. Mater.* 16 (2004) 2300-2308.
- [29] J.C. Rodríguez-Cabello, A. Girotti, A. Ribeiro, F.J. Arias. Synthesis of genetically engineered protein polymers (recombinamers) as an example of advanced self-assembled smart materials. *Methods in molecular biology* 811 (2012) 17-38.
- [30] M. Vallet-Regí, D. Arcos, A. Baeza. Andámio macroporoso cerámico puro basado en apatita nanocrystalina, método de preparación y aplicaciones. Spanish Patent No. ES2373286, 2013.
- [31] A. González-Vázquez, J.A. Planell, E. Engel. Extracellular calcium and CaSR drive osteoinduction in mesenchymal stromal cells. *Acta Biomater.* 10 (2014) 2824-2833.

-
- [32] A. Nakamura, Y. Dohi, M. Akahane, H. Ohgushi, H. Nakajima, H. Funaoka, Y. Takakura. Osteocalcin secretion as an early marker of *in vitro* osteogenic differentiation of rat mesenchymal stem cells. *Tissue Eng. Part C* 15 (2009) 169-180.
- [33] E. Tejeda-Montes, K.H. Smith, E. Rebollo, R. Gómez, M. Alonso, J.C. Rodríguez-Cabello, E. Engel, A. Mata. Bioactive membranes for bone regeneration applications: Effect of physical and biomolecular signals on mesenchymal stem cell behavior. *Acta Biomater.* 10 (2014) 134-141.